ELSEVIER

Catalysis Today 71 (2001) 55–67

CATALYSIS TODAY

www.elsevier.com/locate/cattod

Catalytic dehydrocondensation of methane towards benzene and naphthalene on transition metal supported zeolite catalysts: templating role of zeolite micropores and characterization of active metallic sites

Yuying Shu, Masaru Ichikawa*

Catalysis Research Center, Hokkaido University, Kita-ku N-11, W-10, Sapporo 060-0811, Japan

Abstract

The catalytic dehydrocondensation of methane to benzene and naphthalene with a bulky of hydrogen on transition metal supported zeolite catalysts is one of strategies for the catalytic conversion of methane and a challenging topic in heterogeneous catalysis. This paper is dealt with the current progress in catalytic dehydrocondensation of methane towards benzene and naphthalene on transition metal supported zeolite catalysts, in terms of templating role of zeolite micropores and metallic sites on Mo and Re supported zeolite catalysts. The effect of zeolite supports and active metallic phases in conjunction with the reaction conditions are discussed. The results of investigation on the carbonaceous deposits and the synergetic effect between the transition metal components and the zeolite supports, as well as, the active species and reaction mechanisms are revealed by the TPO/XPS/FT-IR/EXAFS and solid NMR studies.

Keywords: Catalytic dehydrocondensation; Methane; Benzene; Zeolite; Mo; Re

1. Introduction

With the declining of crude oil reserves, the energy supply is changing from being primarily oil based to become more gas based. Methane is the major component of most natural gas reserves, hence, it is important to investigate the conversion of methane from the potential utilization of natural gas. On the other hand, methane is the most stable and symmetric organic molecule consisting of four C–H bonds with bond energy of 435 kJ/mol, accordingly, the investigation of methane conversion also is a great challenge from the aspect of catalysis science.

A number of strategies are being explored for the catalytic conversion of methane to more useful chemicals and fuels as reviewed by Lunsford [1]. The catalytic conversion of methane can be divided into two groups, which are described as indirect and direct. The indirect processes rely upon the production of synthesis gas, either by reforming reaction or by partial oxidation, followed by Fischer–Tropsch chemistry. For the latter transformation route, methane can be converted to the desired products, e.g. ethylene, methanol, formaldehyde, and aromatics, directly. To date, the greatest potential for advance in methane conversion technology is the discovery of direct transformation route for the formation of methanol and formaldehyde [2–4]. The oxidative coupling of methane as an alternative route for the direct conversion of methane had been extensively studied since 1982. The splitting of

* Corresponding author. Tel.: +81-11-706-2912; fax: +81-11-706-4957.
E-mail address: michi@cat.hokudai.ac.jp (M. Ichikawa).

0920-5861/01/$ – see front matter
PII: S0920-5861(01)00440-0

C–H bond is likely from the interaction between CH_4 and the surface oxygen species [5]. A C_2 selectivity of 80% with a CH_4 conversion of 20% can be obtained over SrO/La_2O_3 [6] and $Mn/Na_2WO_4/SiO_2$ [7] catalysts. However, no catalysts could reach C_2 yield above 25% and selectivity to C_2 higher than 80%, and thus limit its industrial application.

Many processes related with methane conversion, whether direct or indirect route, require the use of oxygen, so the deep oxidation of methane is unavoidable. In order to suppress the formation of undesirable products such as CO and CO_2, many researchers tried to transform methane into higher hydrocarbons in the absence of oxygen. Mitchell and Wanyhorne [8] reported that methane could be activated over $M/M'On/M''O$ multi-component catalyst at 977 K to form benzene and/or the carbonaceous deposit. Belgued et al. [9] demonstrated that methane could be transformed into higher hydrocarbons over a supported Pt catalyst via a two-step route. Bragin et al. [10] found the aromatization reaction of methane to benzene over $Pt–CrO_3$/HZSM-5 catalyst at 1023 K in a pulse-reactor.

In 1993, Wang et al. [11] reported that methane could be transformed to benzene in a flow mode reactor on transition metal ions supported HZSM-5 catalysts under non-oxidative condition. Since then, many research groups concerned this catalytic process and made inspiring efforts. Up to now, the research work on this reaction can be sorted into the following parts. (1) Catalyst modification in terms of templating role of zeolite micropores and metallic sites in conjunction with optimization of reaction conditions. (2) Study of the carbonaceous deposits focusing on the coke suppression and characterization. (3) Synergetic effect between the metallic sites and the zeolite supports. (4) Study of the active phases and reaction mechanisms. Hereafter, we will focus on these aspects to present the current advances in catalytic dehydrocondensation of methane towards benzene and naphthalene over transition metal supported zeolite catalysts.

2. Catalyst modification in terms of templating role of zeolite micropores and metallic sites

Many researchers have tried a lot of catalysts, in order to improve the catalyst activity, selectivity and stability as summarized in [12]. It is generally accepted that the Mo/HZSM-5 is one of the good catalysts as reported by groups of Xu and co-workers [13,14], Chen et al. [15], Solymosi et al. [16–19], Wang et al. [20,21], and Liu et al. [22,23]. It is important to note the results reported by Wang et al. [20,21] and Liu et al. [22,23], they noticed and analyzed the production of naphthalene and quantitatively on-line calculated the coke formation by using the internal standard of N_2 and Ar. It also should be noticed that the coke evaluation from GC analysis consists of all the undetected carbon products such as amorphous and graphitic inert carbons that are difficult to detect and analyze with on-line gas chromatographs. In order to look at undetected carbon species, Liu and co-workers [23,24] analyzed all the condensable products in the effluent gas separated for 4 h by using the ethanol-dry ice trap in the methane reaction at 973 K on 3% Mo/HZSM-5 catalyst. The collected reaction products were analyzed by the GC/MS with a capillary column (OV-1, 25 m) up to 553 K and TOFRM (time-of-flight reflect-mass) spectrometer. The results show that a list of aromatic compounds, such as benzene and naphthalene as the major products, and other polycondensed aromatics, such as anthracene, pyrene, tetracene, and their deriviates which were collected as products of the methane reaction. Lu et al. [25] testified the internal standard analysis method by the data of material balance from a 20 ml bench scale reactor.

Weckhuysen et al. [26] studied the effect of transition metal ions, the preparation and treatment method. They found that the activity is in the following sequence: Mo > W > Fe > V > Cr. Later, Zeng et al. [27] reported the $W–H_2SO_4$/HZSM-5 was a good catalyst for methane aromatization at 1123 K, however, the formation of coke was neglected. On the other hand, it should be noted that the addition of a second metal component is also studied as shown in [12]. The improvement in enhancing activity or stability has been obtained by addition with Fe, Co, W, Zr, Ru and Cu [22,28–31].

During the past 8 years, the catalyst modification in term of zeolite micropores was extensively studied [23,32–37]. Some of typical results are listed in Table 1. Zhang et al. studied the methane aromatization over Mo-based catalysts supported on different types of zeolites [32]. It was found that H-type silica–alumina zeolites, such as ZSM-5, ZSM-8, ZSM-11 and β

Table 1
The reaction results of Mo loaded catalysts using various supports for methane dehydrocondensation reaction

Samples	Temperature (K)	SV (ml/g h)	Methane conversion (%)	Selectivity (%)				Reference
				C_2	Benzene	Naphthalene	Coke	
3% Mo/HZSM-5	973	1600	6.9	4.5	91.3	–	–	[32]
6% Mo/HZSM-8	973	1600	4.1	3.9	86.7	–	–	[32]
3% Mo/HZSM-11	973	1600	7.6	5.3	91.6	–	–	[32]
7% Mo/H-β	973	1600	3.1	8.8	80.4	–	–	[32]
3% Mo/HMCM-41	973	1600	0.9	8.7	80.1	–	–	[32]
3% Mo/HSAPO-34	923	1600	0.6	10.1	72.9	–	–	[32]
3% Mo/HZSM-5	973	1440	9.4	2.8	40.9	16.9	36.1	[23]
3% Mo/mordenite	973	1440	7.3	3.5	4.1	0	83.1	[23]
3% Mo/USY	973	1440	6.4	2.2	10.5	0	84.3	[23]
3% Mo/FSM-16	973	1440	6.8	2.2	6.6	0	87.7	[23]
3% Mo/Al_2O_3	973	1440	7.4	2.1	4.0	0	88.9	[23]
6% Mo/HZSM-11	973	1440	8.2	2.4	44.5	11.3	37.2	[33]
6% Mo/H-β	973	1440	6.7	3.6	14.2	2.5	71.5	[33]
6% Mo/nano-HZSM-5	973	1500	6.8	3.4	48.0	12.3	26.3	[34]
6% Mo/micro-HZSM-5	973	1500	10.5	3.2	56.2	16.8	18.9	[34]
6% Mo/HZRP-1	973	1500	10.5	2.3	50.7	29.1	12.5	[35]
15% Mo/HZRP-1	973	1500	10.1	2.4	51.0	17.9	17.3	[35]
6% Mo/HZSM-5	973	1500	10.6	3.3	57.8	19.8	18.1	[36]
6% Mo/HMCM-22	973	1500	10.0	3.4	80.0	4.4	12.0	[36]

possessing two-dimensional structure and pore diameter equaling the dynamic diameter of a benzene molecule, are fine supports for methane dehydroaromatization catalysts. Liu et al. [23] studied the direct conversion of methane to aromatics on a series of Mo supported catalysts using HZSM-5, FSM-16, mordenite, USY, SiO_2, and Al_2O_3 as the supporting materials based on the total carbon balances. Among all the supports used, the HZSM-5 supported Mo catalysts exhibit the highest yield of aromatic products, achieving over 70% selectivity of total hydrocarbons at 5–12% methane conversion at 973 K. Recently, the further study on the templating role of zeolite micropores was reported [33]. It was concluded that the zeolites having pore size of 5–6 Å, similar as the kinetic diameters of benzene and naphthalene molecules are good carriers.

Zhang et al. [34] investigated the catalytic performance of Mo supported microsized and nanosized HZSM-5 zeolites. The catalytic performance of Mo/micro-HZSM-5 is better than that of Mo/nano-HZSM-5. Recently, Shu et al. report that HZRP-1 zeolite, a kind of phosphoric and rare earth oxide-containing penta-sil type high-silica zeolite, was a good support for methane dehydroaromatization catalyst [35]. Compared with Mo/HZSM-5 catalysts, Mo/HZRP-1 catalysts are more active at high Mo loading. Finally, they found Mo/HMCM-22 was a highly selective catalyst for benzene formation in methane dehydroaromatization [36]. The selectivity to light aromatics of 80% at a CH_4 conversion of 10.0% was obtained on 6% Mo/HMCM-22 at 973 K. The

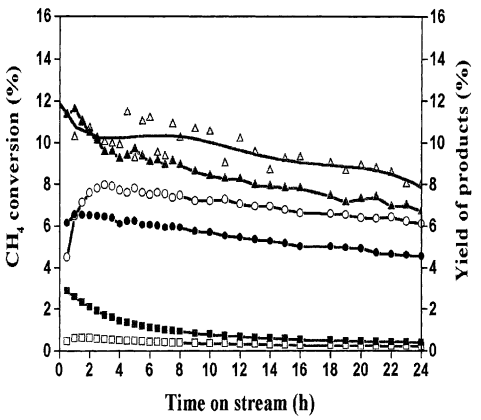

Fig. 1. A comparison of the changes of methane conversion (△), yield of benzene (○), and yield of naphthalene (□) vs. time on stream on 6Mo/MCM-22 (open symbols) and 6Mo/HZSM-5 (solid symbols) [37].

comparative reaction results on Mo/HMCM-22 and Mo/HZSM-5 catalysts are shown in Fig. 1 [37]. The catalytic performance on Mo/HMCM-22 is featured with a higher yield of benzene and a lesser yield of naphthalene in comparison with that on Mo/HZSM-5 catalyst. In addition, it was found that more coke formed on Mo/HMCM-22 catalyst. They proposed the catalytic feature on the Mo/HMCM-22 catalyst be mainly related with its unique pore system. The typical framework structure of MCM-22 and ZSM-5 zeolites are presented in Fig. 2. For ZSM-5 zeolite, it possesses a two-dimensional channel system which consists of straight channels running parallel to [0 1 0], having 10-ring of 5.3 × 5.6 Å free diameter, as well as sinusoidal channels running parallel to [1 0 0], having 10-ring of 5.1 × 5.5 Å free diameter. For MCM-22 zeolite, its topological structure is composed of an interconnected building unit forming two independent pore systems: two-dimensional sinusoidal 10-ring interlayer channels of 4.0 × 5.9 Å and 12-ring interlayer supercages of 7.1 × 18.2 Å with 4.0 × 5.4 Å entrance aperture. The relatively smaller size of pore mouth of MCM-22 may contribute to its higher benzene selectivity than that of ZSM-5. On the other hand, large numbers of 7.1 × 18.2 Å cavities existed on MCM-22 zeolite was contributed to its higher coke tolerance than that of ZSM-5 zeolite.

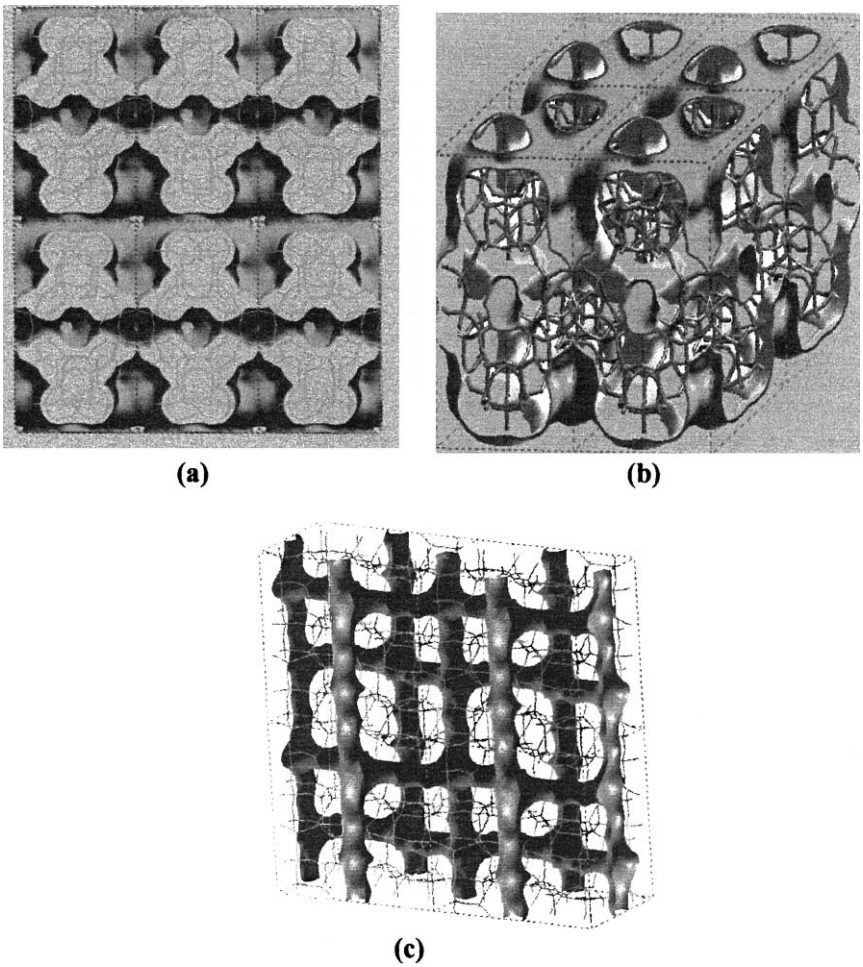

Fig. 2. The framework structure of MCM-22 zeolite (a, b) and ZSM-5 zeolite (c).

The previous studies had demonstrated that, besides Mo active component, only transition metals such as Fe, V, Co, and W showing slight activity of methane to aromatics were reported before 1999 [23,26,27,29]. Recently, Wang et al. [38,39] reported a novel and promising system of Re/HZSM-5 for the catalytic dehydrocondensation of methane. Representative result is shown in Fig. 3. It was found that C_2 hydrocarbons and aromatic compounds such as benzene and naphthalene were continuously obtained with a considerable evolution of hydrogen. The results on the Re/HZSM-5 show that the benzene selectivity based on the consumed methane exceed 65% at the maximum value, due to the modest formation of coke and polycondensed byproducts. Similar to Mo/HZSM-5 catalyst, high methane conversion and formation rate of benzene was achieved on the Re/HZSM-5 catalyst.

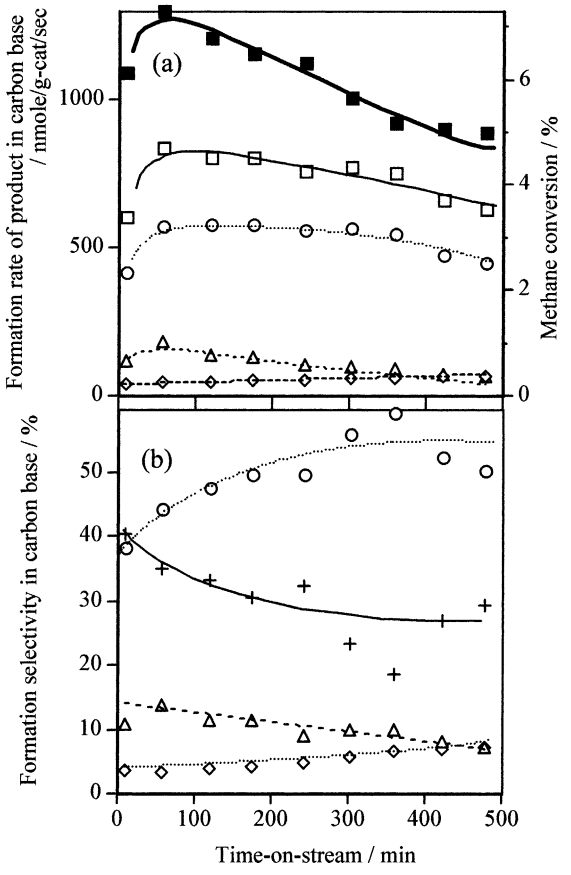

Fig. 3. Catalytic performance of 5Re/HZSM-5 in the dehydrocondensation of methane at 973 K, 3 atm, and 1440 ml/g cat/h of methane space velocity: (a) rates of product formation and of methane conversion; and (b) formation selectivities in the methane consumed vs. time on stream, where (■) refers to both the methane conversion rate and methane conversion percent. Symbols (□), (◇), (○), (△), and (+) refer to the formation rate of product and the formation selectivity of hydrocarbons, ethane + ethene, benzene, naphthalene, and coke, respectively [38].

In addition, optimization of reaction conditions had also been studied. The experimental results showed that various pretreatment and different reaction conditions exerted great influence on the catalytic performance as summarized in [12]. Pierella et al. [40] and Choudhary et al. [41] studied the effect of the presence of light hydrocarbons in the methane feed. They all observed the conversion of methane at the lower temperatures (673–873 K). Recently, Borry et al. [42] investigated the non-oxidative catalytic conversion of methane with continuous hydrogen removal by simulation of membrane reactors. They suggested that the removal of H_2, perhaps by membrane separation, would shift the equilibrium of the methane dehydroaromatization and allow the higher conversion of methane to be achieved.

3. Study of the carbonaceous deposits

The heavy carbonaceous deposit formed in methane dehydrocondensation is a major obstacle for a better understanding of the reaction and its practical utilization. Ichikawa and co-workers [24,43,44] reported the unique promotional effect of CO and CO_2 on the catalytic stability for benzene and naphthalene production on Mo/HZSM-5 and Fe/Co-modified Mo/HZSM-5 catalyst owing to the efficient suppression of coke formation. The representative results are plotted in Fig. 4. For Co modified Mo/HZSM-5 catalyst the methane reaction with CO yields higher activities (950–1000 nmol/g cat/s in carbon base) of benzene production with good stability for more than 100 h due to the minimization of the coke formation to less than 20%. By contrast, the activity of the catalyst decreased greatly under pure methane feed at the same reaction conditions. Similarly, the stability of the catalyst was also improved by adding a few per cent CO_2 into the methane feed gas. It is demonstrated that added CO_2 is converted to 2 mol of CO by the reforming process ($CO_2 + CH_4 = 2CO + 2H_2$) or by the reverse Boudart reaction ($CO_2 + C = 2CO$).

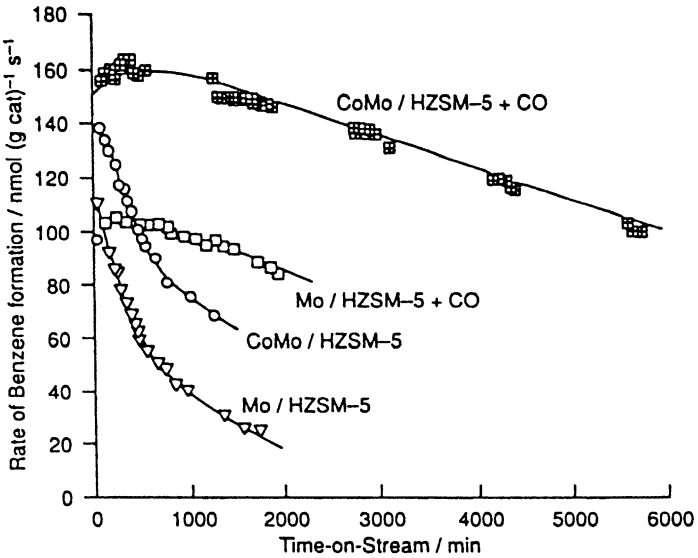

Fig. 4. Rates of benzene formation in methane aromatization reaction on 3% Mo/HZSM-5 (▽) and 1% Co, 3% Mo/HZSM-5 (○) catalysts using pure methane and on 3% Mo/HZSM-5 (□) and on 1% Co, 3% Mo/HZSM-5 (⊞) using methane + 4% CO at 973 K and 1 atm [44].

^{13}CO isotopic labeling tracer studies [24] demonstrated that ^{13}C from ^{13}CO is easily incorporated into methane and products such as benzene and ethylene. The unique role of CO addition to methane feed is based on the formation of minute amounts of CO_2 and C by the Boudart reaction, where C is hydrogenated to a common active carbon species [CH_x] involving methane conversion toward aromatic products such as benzene and naphthalene, while CO_2 reacts with the surface inert carbon species (coke) to regenerate CO, resulting in improved catalyst stability due to efficient suppression of coke formation on the catalyst.

Yuan et al. [45] studied the effect of oxygen on the methane dehydroaromatization over the Mo/HZSM-5 catalyst and found that the small amount of oxygen is beneficial to improve the durability of the catalyst. They suggested that the small amount of O_2 partly removes the coke deposits on the active sites and keeps the catalyst as MoO_xC_y/HZSM-5. Lu et al. [25] found that the pretreatment on HZSM-5 zeolite by steams reduced the serious deposition of coke on Mo/HZSM-5 catalyst.

Weckhuysen et al. [46] characterized the surface carbon formed during the methane conversion on Mo/HZSM-5 catalysts by XPS technique. They identified three different types of surface carbon species existed, which denoted as species A, B, and C, respectively. Species A, with a C_{1s} bonding energy (BE) of 284.6 eV, was due to graphitic-like carbon. Species B, with a C_{1s} BE of 282.7 eV, was due to carbidic-like carbon in Mo_2C. Species C, with a C_{1s} BE of 283.2 eV was a hydrogen-poor sp-type or pre-graphitic type of carbon. It was suggested that the sp-type carbon gradually covers both the zeolite surface and the Mo_2C phase during methane activation and is responsible for the deactivation of Mo/HZSM-5 catalyst in methane dehydroaromatization.

Jiang et al. [47] studied the carbonaceous deposits on Mo/HZSM-5 catalyst by NMR technique. They indicated that there are two kinds of carbonaceous deposits, one is located on partially reduced Mo species and the other is on acid sites of zeolite. The former is responsible for methane activation and transformation from cabene-like species and/or carbide species to ethylene. The latter is active for the formation of aromatics from ethylene. Yuan et al. [45] characterized the carbonaceous deposits by UV-Raman spectroscopy, and disclosed that the carbonaceous deposits formed on Mo/HZSM-5 is mainly polyaromatic.

Ichikawa and co-workers [24,39,44] studied the carbonaceous deposits formed on the catalyst surface in methane aromatization without or with CO/CO_2

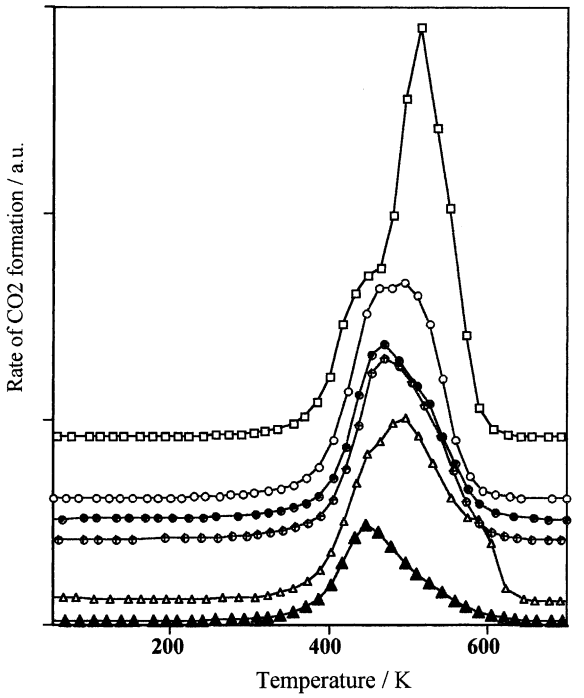

Fig. 5. TPO patterns of 3% Mo/HZSM-5 catalyst after methane aromatization reaction running for 6 h at 973 K and 1 atm pressure with different amounts of CO or CO_2 added to methane feed gas. CH_4 (□), +1.7% CO (○), +4% CO (●), +12% CO (⊕), +1.6% CO_2 (△), +4% CO_2 (▲) [24].

addition by TPO experiment. Some typical results are depicted in Fig. 5. It was demonstrated that there are mainly two kinds of coke produced and the coke amount was greatly reduced by adding various amounts of CO or CO_2 to the methane feed gas. The increase in CO concentration from 1.7 to 12.0% in methane flow resulted in a marked suppression of the total coke formation, particularly the irreversible or inert coke which was oxidized to CO_2 at the higher temperature above 773 K in TPO experiment. On the other hand, the CO_2 addition (1.6–4%) to methane feed effectively reduced both the inert and the reactive coke, as a result, leaving a small amount of the reactive coke, which is oxidized at temperatures lower than 690 K. These TPO data are consistent with the catalytic performance of methane aromatization by addition of CO_2 to methane feed, different from those of CO addition.

Recently, Ma et al. [48] studied the coked Mo/HMCM-22 sample by TPO technique. There are two peaks located at 742 and 830 K were observed, implying that at least two kinds of coke exist on the catalyst surface. It was suggested that the deactivation of the catalysts be mainly due to the carbonaceous deposits on the zeolite acid sites. Finally, Ding et al. [49] studied the evolution of CO_x and H_2O when samples used for CH_4 reactions are treated in 40% O_2/He and the temperature is increased from room temperature to 973 K. Three CO_x peaks were detected. They assigned these peaks to the combustion of (1) carbidic carbon in MoC_x; (2) carbonaceous species within zeolite channels near Mo species that catalyze O_2 dissociation step; and (3) carbon deposits distant from these Mo species.

4. Synergetic effect between the metallic sites and the zeolite supports

The synergetic effect between the metallic sites and the zeolite supports is of significance for the better understanding of methane dehydrocondensation reaction. Xu et al. [50] characterized the interaction between ammonium heptamolybdate and NH_4ZSM-5 zeolite at different stages of catalyst preparation by FT-IR and different TP techniques. The results showed that if Mo/HZSM-5 catalysts were calcined at a proper temperature, the Mo species would interact with acid sites (mainly with Brönsted acid sites) and part of the Mo species will move into the channel. If it is calcined at 973 K, a strong interaction between the Mo species and the skeleton of HZSM-5 will occur accompanying the formation of MoO_4^{2-} species, which is detrimental to methane activation. The group of Xu et al. [51] also investigated the active Mo species by NH_4OH extraction combined with XRD, NH_3–TPD and TPR analyses. Further they studied the interaction by solid NMR with a ^{27}Al and ^{29}Si probe [52]. The results showed that there is a strong interaction between the Mo species and the framework Al and this kind of interaction could lead to the extraction of the framework Al.

Solymosi et al. [16–19] and Wang et al. [20,21] conducted XPS, ion-scattering spectroscopy (ISS) and FT-IR measurements on the Mo/HZSM-5 catalyst. The Mo species in a sample calcined at 403 K

was mainly presented as small (30–50 Å) crystallites of the original ammonium heptamolybdate. After calcination at higher temperature (773–973 K), the Mo species became more highly dispersed on the external surface. During preparation, a portion of the Mo ions diffused into the channels. The FI-IR spectra showed that the intensities of three stretching bands at 3747, 3611 and 3670 cm^{-1} diminished with the introduction of Mo on HZSM-5 zeolite, demonstrating the interaction between Mo and zeolite support. Zhang et al. [53] found the direct evidence for migration of molybdenum into the zeolite pores during calcination at high temperature by FT-IR, ^{27}Al and ^{29}Si NMR experiments.

Liu and co-workers [23,43] studied the bifunctional catalysis of Mo/HZSM-5 in the dehydrocondensation of methane by XAFS/TG/DTA/MASS/FT-IR characterizations. The TG/DTA/MASS and EXAFS studies reveal that the Mo oxide supported on HZSM-5 is endothermically converted with methane at 955 K to molybdenum carbide Mo_2C, which initiates the methane conversion around 960 K, yielding benzene, naphthalene, and C_2 hydrocarbons. The IR measurements in pyridine adsorption reveal that Mo/HZSM-5 catalysts having the optimum SiO_2/Al_2O_3 ratio between 20 and 70 show the maximum Brönsted acidity. A remarkable synergetic promotion in benzene formation exists for the hybrid catalysts consisting of 3% Mo/SiO_2 + HZSM-5 and Mo_2C + HZSM-5, whereas each component by itself shows marginal activity in the reaction. They discussed the bifunctional catalysis by analogy with the promotion mechanism on the Pt/Al_2O_3 catalyst for the dehydroaromatization of alkanes.

Iglesia and co-workers [54,55] investigated the structure of Mo and acid sites in Mo-exchanged HZSM-5 catalyst by stoichiometry of the solid-state exchange reaction. The amount of H_2O evolved during the exchange and the amount of residual OH groups detected by isotopic equilibration with D_2 showed that each Mo atom replace one H^+ during exchange. This stoichiometry and the requirement for charge compensation suggests that exchanged species consist of $(Mo_2O_5)^{2+}$ ditetrahedral structures interacting with two cationic exchange sites. Li et al. further studied the structure of MoO_x and MoC_y in Mo/HZSM-5 catalyst by in situ Raman and X-ray adsorption spectroscopy (XAS) [56]. Finally, they described the recent results dealing with the reduction, carburization, and migration of Mo species during methane reaction [49]. It was reported that the reduction and carburization of $(Mo_2O_5)^{2+}$ species on Mo/HZSM-5 cause the formation of MoC_x particles and the concurrent regeneration of the bridging OH groups initially displaced by the Mo oxo dimers during exchange.

Ma et al. [57] studied the interaction between Mo species and HZSM-5 zeolite by ESR technique. Four different EPR signals, denoted as signals A, B, D, and E, respectively, have been recorded on the Mo/HZSM-5 sample during its reduction by methane. There are two kinds of Mo species observed on the Mo/HZSM-5 sample, the first kind is polynuclear and located on the external surface, while the second kind is associated with the Al in the lattice channels of the zeolite. The hyperfine EPR signals of migrating Mo ion (signals D and E) demonstrated the intense interaction between the Mo species and the lattice Al atom.

Bao and co-workers investigated the synergetic effect between Mo and zeolite supports on Mo modified HZSM-5 [34,58–60], HZRP-1 [61] and HMCM-22 [62] catalysts by in situ MAS NMR technique. The interaction between Mo species and zeolite support was so strong that the framework aluminum could be extracted, accompanied by the formation of $Al_2(MoO_4)_3$ crystallines. ^{27}Al MAS NMR spectra in the calcined and reacted Mo/HZRP-1 catalysts [61] revealed that the presence of tetrahedral framework aluminum, which is associated with the formation of Brönsted acidic sites, is of great significance for methane dehydroaromatization. Finally, they firstly observed the variation of the amount of Brönsted acid sites during a real methane dehydroaromatization reaction, as well as the formation of water, benzene, and aromatic carbonaceous deposits by in situ ^1H MAS NMR spectroscopy [60]. The representative ^1H MAS NMR spectra of 6% Mo/HZSM-5 are presented in Fig. 6. As shown, on increasing the temperature to 973 K for 10 min, the Brönsted acid signal at $\delta = 4.1$ decreased drastically, and two new resonance at $\delta = 6.8$ and 7.9 emerged clearly when the reaction time was prolonged. The peak at $\delta = 6.8$ is assigned to the water molecules formed and adsorbed during the reaction, whereas the signal at $\delta = 7.9$ is assigned to the hydrogen atoms of the aromatic species that are

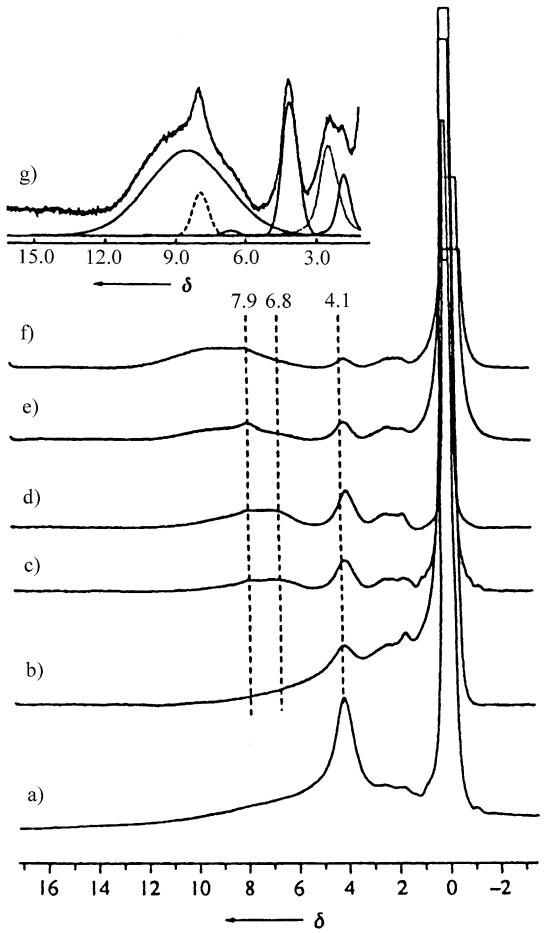

Fig. 6. ^{1}H MAS NMR spectra of 6% Mo/HZSM-5 treated with (a) methane flow at 873 K for 1 h; after the methane dehydroaromatization reaction (973 K, 1500 ml g^{-1} h^{-1}, 1 atm) reaction times: (b) 10 min; (c) 30 min; (d) 1 h; (e) 3 h; (f) 6 h. Spectrum (g) is an expansion of spectrum (e), with six lings simulating the original spectrum [60].

produced on the aromatization centers of the Brönsted acid sites. This gives a vivid description of what has happened on the catalyst surface during the methane dehydroaromatization than data from the gas phase analysis.

5. Active species and reaction mechanisms

The mode of methane activation is one of hot topics concerned with methane dehydrocondensation and many kinds of active sites and reaction mechanisms have been proposed. By X-ray photoelectron spectroscopy (XPS) technique, Solymosi et al. [16,17] found Mo_2C was formed on the used catalyst and regarded this as the active species. Further they studied the catalytic performance of unsupported and supported Mo_2C [18,19] and concluded that, besides Mo_2C, the presence of the oxygen deficient MoO_2 probably was also responsible for the methane activation.

Wang et al. [20,21] also characterized the Mo/HZSM-5 catalyst by XPS technique and found that during the initial induction period, CH_4 reduced the Mo^{6+} in the zeolite to Mo_2C accompanied by carbonaceous deposits. Pretreatment of the catalyst in a CH_4/H_2 gas mixture at 973 K reduces Mo^{6+} ions in the calcined catalyst into Mo_2C and almost eliminates the induction period, confirming that Mo_2C is the active species in the activation of methane. They found that pre-formation of Mo_2C, without coke deposit, could not completely eliminate the induction period. So they suggested that a coke modified Mo_2C might be the active species in the formation of ethylene.

Surrounding the study of the active species, XPS, TPR, DTA, EPR, MASS and simulation study were successively used by the group of Xu and Bao [29,30,48,57,63]. By EPR technique, Ma et al. [57] proposed that the fully reduced Mo_2C species resulted from the MoO_3oct species crystallites and the MoO_xsqu species, and the partially reduced Mo species formed from the Mo species associated with the Al atom are responsible for methane dehydroaromatization. They also investigated the nature of the induction period as well as the environment needed for methane aromatization over different Mo-based catalysts by TP technique [48]. It was demonstrated that the molybdenum carbide, which can continuously activate methane even when multiple layers of carbonaceous species are formed on its surface, and Brönsted acid sites, to which the activated intermediate can migrate, together with the particular channel structure of zeolite, are key roles for methane dehydroaromatization. Recently, Zhou et al. performed Monte Carlo calculation simulation study on the absorption of molybdenum species in the channels of HZSM-5 zeolite [63]. Two models of mobile Mo species were designed and their sorption in HZSM-5 zeolite pores were investigated. The simulation

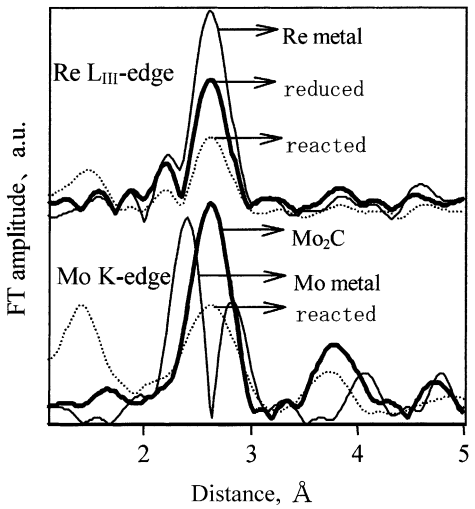

Fig. 7. Mo K-edge and Re L_{III}-edge FT spectra of Mo metal, Mo_2C and reacted Mo/HZSM-5 (bottom), Re metal, reduced and reacted Re/HZSM-5 (top), respectively [23,39].

calculation results suggest that the tetrahedral co-ordinated $MoO_2(OH)_2$ should be possible mobile Mo species in ZSM-5 zeolite pores.

To characterize the active phase and elucidate the mechanism of methane dehydrocondensation to benzene, Mo K-edge EXAFS and TG/DTA/MASS/FT-IR techniques were used by Ichikawa and co-workers [23,38,39,43]. The representative EXAFS results are shown in Fig. 7. The FT function of the Mo/HZSM-5 samples reacted with the methane at 973 K showed peaks at the same position as those for the Mo_2C reference. After the reaction with methane, the Mo oxide species is converted with methane to Mo_2C cluster (Mo–Mo: CN = 2.1–2.5, R = 2.96–2.98 Å; Mo–C: CN = 0.8–0.9, R = 2.12–2.14 Å), in comparison with those of the Mo_2C reference (Mo–Mo: CN = 12, R = 2.97 Å; Mo–C: CN = 3, R = 2.10 Å) [23,43]. The XANES/EXAFS and TG/DTA/MASS studies reveal that the zeolite supported Mo oxide is endothermally converted to molybdenum carbide (Mo_2C) cluster under methane, which initiates the methane aromatization to benzene and naphthalene at 873–1023 K. On the other hand, it was demonstrated that there is a close correlation between the activity of benzene formation in methane aromatization and the Brönsted acidity of Mo/HZSM-5 catalyst. These results suggest that methane is dissociated on the molybdenum carbide cluster supported on HZSM-5 having optimum Brönsted acidity to form CH_x ($x > 1$) and C_2-species as the primary intermediates which are subsequently oligomerized to aromatics such as benzene and naphthalene at the interface of Mo_2C and HZSM-5 zeolite having the optimum Brönsted acidity. The main transformation steps of this process could be outlined as follows:

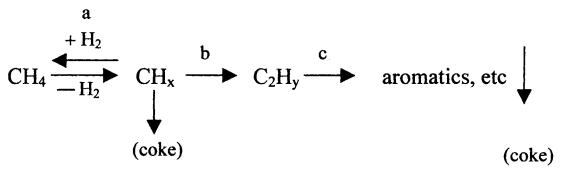

where (a–b) are on an Mo site of carbide or oxycarbide and (c) is on HZSM-5.

Recently, the group of Ichikawa et al. further investigated the active species on Re/HZSM-5 catalyst by EXAFS technique coupled with TG/DTA/MASS [38,39]. As presented in Fig. 7, the FT functions of the Re/HZSM-5 samples reduced at 573 K, reacted with methane at 973 K are similar in the shape with those of Re metal powder. EXAFS parameters of the samples showed that after the reduction or reaction, Re oxide species is converted to Re particle (Re–Re: R = 2.74 Å, CN = 4.0) in comparison with those of Re metal powder (Re–Re: R = 2.74 Å, CN = 12). TG/DTA/MASS and EXAFS studies revealed that the Re oxide species dispersed in the calcined HZSM-5 is reduced with hydrogen at 573 K or reacted with methane at 895 K to metallic Re. In contrast to the molybdenum carbide (Mo_2C) as the active species for methane dehydrocondensation over the Mo/HZSM-5 catalyst, it was presented that the metallic Re on Re/HZSM-5 is responsible for the catalytic dehydrocondensation of methane toward C_2 hydrocarbons and benzene and naphthalene.

Iglesia and co-workers studied the Mo species in Mo-exchanged HZSM-5 catalyst for non-oxidative methane conversion by measurements of the kinetics of formation and of the stoichiometry of exchanged MoO_x species and in situ Raman study [54–56]. Recently, they investigated the structure and density of molybdenum species in Mo/HZSM-5 during the catalytic CH_4 reaction by in situ XAS, temperature-programmed oxidation after reaction, and the isotopic exchange of D_2 with OH groups in

HZSM-5 before and after CH_4 reaction [49]. These methods reveal that methane reaction cause exchanged $Mo_2O_5^{2+}$ dimers to reduce and carburize to form small MoC_x (0.6–1 nm) clusters with the concurrent regeneration of the bridging OH groups that were initially replaced by Mo oxo dimers during exchange. In this manner, catalytically inactive Mo oxo species activate in contact with CH_4 to form the two sites required for the conversion of CH_4 to aromatics: MoC_x for C–H bond activation and initial C–C bond formation and acid sites for oligomerization and cyclization of C_{2+} hydrocarbons to form stable aromatics.

6. Prospective aspects for methane dehydrocondensation process

Methane dehydrocondensation in the absence of oxygen over transition metal ions (mainly Mo, Re) supported zeolite catalysts has been extensively studied since first report in 1993. During the past 8 years, several important progresses were fulfilled. For catalyst evaluation, many research groups had established the more accurate analysis systems. With the use of N_2 and Ar as an internal standard, the carbonaceous species formed was on-line calculated, so the reaction result of the catalyst is more reliable. Up to date, some novel catalysts were reported, it can be concluded that Mo and Re are the good active metal components, while HZSM-5, HMCM-22, HZSM-11 and HZRP-1 are the fine zeolite supports. It is recognized that the methane dehydrocondensation reaction needs bifunctional catalyst and the zeolites with two-dimensional structure and pore size near to the dynamic diameters of benzene and naphthalene molecules are fine supports. For the improvement of the catalyst activity and stability, Ichikawa and co-workers have shown that the addition of small amounts CO and CO_2 to the methane feed inhibits the deactivation of the catalyst greatly. The synergetic effect between the Mo species and zeolite supports are thoroughly investigated by FT-IR, XPS, EPR, solid NMR, EXAFS, stoichiometry of the solid-state exchange reaction, and in situ Raman techniques. It had been accepted that the interaction between Mo and the zeolite support is very important both in the preparation of a good catalyst and in the catalytic reaction process. Generally speaking, the active metal species and the Brönsted acidity of the zeolite as well as the channel structure are crucial factors for the catalytic performance. It is basically agreed that molybdenum carbide or oxycarbide is the active species for the activation of C–H bond of methane, then the formed intermediate is transformed to aromatic products on the acidic sites within the channels of the zeolite. By contrast, for Re supported HZSM-5 catalyst, it was presented that the metallic Re is responsible for methane activation based on EXAFS and TG/DTA/MASS studies.

Although a lot of research work had been done, in terms of catalyst preparation, characterization, coke formation and reaction mechanism, some problems still remain to be solved, not only from the aspect of fundamental research, but also from the aspect of practical utilization of methane dehydrocondensation. Some key points for prospective research on methane dehydrocondensation are described as following.

6.1. The achievement of high activity and stability

In order to achieve the high activity and stability in methane dehydrocondensation, the following methods should be considered.

1. Improvement of the catalyst
   Some new catalysts, both from the zeolite supports and the active metal components, need to be discovered. On the other hand, try to modify the previous catalysts by addition of certain elements and optimization of the preparation and pretreatment methods.
2. Removal of H_2 by membrane technique
   As previously presented by Borry et al. [42], the removal of H_2 is one of the efficient ways for the overcoming of the thermodynamic and kinetic limit in methane dehydrocondensation. Therefore, the study of membrane reactor for H_2 removal is needed.
3. Adoptions of integrated recycle reaction system
   As reported by Qiu et at. [64], methane can be converted in high yields to aromatics using an integrated recycle system containing both an oxidative coupling reactor at 1073 K, for conversion of CH_4 to C_2H_4, and a secondary reactor containing Ga/ZSM-5 at 793 K for subsequent conversion of ethylene to aromatics. Using this system, the aromatic product yields of >70% at CH_4 conver-

sion of ~100%, based on total added CH_4, can be obtained. Therefore, the study on the integrated recycle reaction system was necessary for the achievement of high activity and stability, especially from the potential commercialized aspect of this reaction.

6.2. The effect of channel structure

The previous studies had shown that with the use of different zeolite as catalyst support, such as HMCM-22 and HZSM-5, the formation distribution of benzene, naphthalene and coke is quite different. However, how the channel structure of the zeolite support affect the product distribution and coke formation is still not clear and this kind of study is emerging. It will give us a guide for the preparation of new catalyst and also be useful for the deep understanding of methane dedydrocondensation.

6.3. The nature of carbonaceous deposits

The carbonaceous deposit formed in methane dehydrocondensation is a main obstruction for understanding of this reaction and the development of this process. Unfortunately, this kind of study is scarce. The reason is due to the study on the nature and location of carbonaceous deposit is always tough. Anyway, some studies on this aspect need conducted.

6.4. Active sites and reaction mechanisms

Although several research groups have investigated the active sites by various techniques, it is still controversial in some points, so the further study is needed. For the reaction mechanisms, some of conclusions are still based on the presumption, so the direct evidence for the reaction mechanism needs established.

References

[1] J.H. Lunsford, Catal. Today 63 (2000) 165.
[2] R.A. Periana, D.J. Taube, S. Gamble, H. Taube, T. Satoh, H. Fujii, Science 280 (1998) 560.
[3] R.G. Herman, Q. Sun, C. Shi, K. Klier, C.B. Wang, H. Hu, I.E. Wachs, M.M. Bhasin, Catal. Today 37 (1997) 1.
[4] A. Parmaliana, F. Arena, F. Frusteri, A. Mezzapica, Stud. Surf. Sci. Catal. 119 (1998) 551.
[5] J.H. Lunsford, in: Proceedings of the 10th International Congress on Catalysis, Vol. 69, 1993.
[6] H. Mimoun, A. Robine, S. Bonnaudet, C.J. Cameron, Appl. Catal. 58 (1990) 269.
[7] S. Pak, P. Qiu, J.H. Lunsford, J. Catal. 179 (1998) 222.
[8] H.L. Mitchell III, R.H. Wanyhorne, US Patent, 4 239 658 (1980).
[9] M. Belgued, P. Pareja, A. Amarillo, Nature 352 (1991) 789.
[10] O.V. Bragin, T.V. Vasina, A.V. Preobrazhenskii, Kh.M. Minachev, IZV Ser. Khim. 3 (1989) 750.
[11] L. Wang, L. Tao, M. Xie, G. Xu, J. Huang, Y. Xu, Catal. Lett. 21 (1993) 35.
[12] Y. Xu, L. Lin, Appl. Catal. A 188 (1999) 53.
[13] Y. Xu, S. Liu, L. Wang, M. Xie, X. Guo, Catal. Lett. 30 (1995) 135.
[14] S. Wong, Y. Xu, W. Liu, L. Wang, X. Guo, Appl. Catal. A 136 (1996) 7.
[15] L. Chen, L. Lin, Z. Xu, X. Li, T. Zhang, J. Catal. 157 (1995) 190.
[16] F. Solymosi, A. Erdohelyi, A. Szoke, Catal. Lett. 32 (1995) 43.
[17] F. Solymosi, A. Szoke, J. Cserenyi, Appl. Catal. A 142 (1996) 361.
[18] F. Solymosi, A. Szoke, J. Cserenyi, Catal. Lett. 39 (1996) 157.
[19] F. Solymosi, J. Cserenyi, A. Szoke, T. Bansagi, A. Dszko, J. Catal. 165 (1997) 150.
[20] D. Wang, J.H. Lunsford, M.P. Rosynek, Topics Catal. 3 (1996) 289.
[21] D. Wang, J.H. Lunsford, M.P. Rosynek, J. Catal. 169 (1997) 347.
[22] S. Liu, Q. Dong, R. Ohnishi, M. Ichikawa, Chem. Commun. (1997) 1445.
[23] S. Liu, L. Wang, R. Ohnishi, M. Ichikawa, J. Catal. 181 (1999) 175.
[24] R. Ohnishi, S. Liu, Q. Dong, L. Wang, M. Ichikawa, J. Catal. 182 (1999) 92.
[25] Y. Lu, Z. Xu, Z. Tian, T. Zhang, L. Lin, Catal. Lett. 62 (1999) 215.
[26] B.M. Weckhuysen, D. Wang, M.P. Rosynek, J.H. Lunsford, J. Catal. 175 (1998) 338.
[27] J. Zeng, Z. Xiong, H. Zhang, G. Lin, K. Tsai, Catal. Lett. 53 (1998) 119.
[28] L. Wang, Y. Xu, M. Xie, S. Liu, L. Tao, Stud. Surf. Sci. Catal. 94 (1995) 495.
[29] S. Wong, Y. Xu, L. Wang, S. Liu, G. Li, M. Xie, X. Guo, Catal. Lett. 38 (1996) 39.
[30] Y. Shu, Y. Xu, S. Wong, L. Wang, X. Guo, J. Catal. 170 (1997) 11.
[31] S. Li, C. Zhang, Q. Kan, D. Wang, T. Wu, L. Lin, Appl. Catal. A 187 (1999) 199.
[32] C. Zhang, S. Li, Y. Yuan, W. Zhang, T. Wu, L. Lin, Catal. Lett. 56 (1998) 207.
[33] Y. Shu, R. Ohnishi, M. Ichikawa, D. Ma, L. Xu, Y. Xu, X. Bao, Catal. Catal. 43 (2001) 137.
[34] W. Zhang, D. Ma, X. Han, X. Liu, X. Bao, X. Guo, X. Wang, J. Catal. 188 (1999) 392.

[35] Y. Shu, D. Ma, X. Bao, Y. Xu, Catal. Lett. 66 (2000) 161.
[36] Y. Shu, D. Ma, L. Xu, Y. Xu, X. Bao, Catal. Lett. 70 (2000) 67.
[37] Y. Shu, D. Ma, L. Su, L. Xu, Y. Xu, X. Bao, Stud. Surf. Sci. Catal. 136 (2001) 27.
[38] L. Wang, R. Ohnishi, M. Ichikawa, Catal. Lett. 62 (1999) 29.
[39] L. Wang, R. Ohnishi, M. Ichikawa, J. Catal. 190 (2000) 276.
[40] L.B. Pierella, L. Wang, O.A. Anunziata, React. Kinet. Catal. Lett. 60 (1997) 101.
[41] V.R. Choudhary, A.K. Kinage, T.V. Choudhary, Science 275 (1997) 1286.
[42] R.W. Borry, E.C. Lu, Y.-H. Kim, E. Iglesia, Stud. Surf. Sci. Catal. 119 (1998) 403.
[43] S. Liu, L. Wang, Q. Dong, R. Onishi, M. Ichikawa, Stud. Surf. Sci. Catal. 119 (1998) 241.
[44] S. Liu, L. Wang, Q. Dong, R. Ohnishi, M. Ichikawa, Chem. Commun. (1998) 1217.
[45] S. Yuan, J. Li, Z. Hao, Z. Feng, Q. Xin, P. Ying, C. Li, Catal. Lett. 63 (1997) 73.
[46] B.M. Weckhuysen, M.P. Rosynek, J.H. Lunsford, Catal. Lett. 52 (1998) 31.
[47] H. Jiang, L. Wang, W. Cui, Y. Xu, Catal. Lett. 57 (1999) 95.
[48] D. Ma, Y. Shu, M. Cheng, Y. Xu, X. Bao, J. Catal. 194 (2000) 105.
[49] W. Ding, S. Li, G.D. Meitzner, E. Iglesia, J. Phys. Chem. B 105 (2001) 506.
[50] Y. Xu, Y. Shu, S. Liu, J. Huang, X. Guo, Catal. Lett. 35 (1999) 233.
[51] Y. Xu, W. Liu, S. Wong, L. Wang, X. Guo, Catal. Lett. 40 (1996) 207.
[52] W. Liu, Y. Xu, S. Wong, J. Qiu, N. Yang, J. Mol. Catal. A 120 (1997) 257.
[53] J.Z. Zhang, M.A. Long, R.F. Howe, Catal. Today 44 (1998) 293.
[54] R.W. Borry, Y.-H. Kim, A. Huffsmith, J.A. Reimer, E. Iglesia, J. Phys. Chem. B 103 (1999) 5787.
[55] Y.H. Kim, R.W. Borry, E. Iglesia, Micropor. Mesopor. Mater. 35/36 (2000) 495.
[56] W. Li, G.D. Meitzner, R.W. Borry, E. Iglesia, J. Catal. 191 (2000) 373.
[57] D. Ma, Y. Shu, X. Bao, Y. Xu, J. Catal. 189 (2000) 314.
[58] W. Zhang, X. Bao, X. Guo, X. Wang, Catal. Lett. 60 (1999) 89.
[59] W. Zhang, D. Ma, X. Liu, X. Liu, X. Bao, Chem. Commun. (1999) 1091.
[60] D. Ma, Y. Shu, W. Zhang, X. Han, Y. Xu, X. Bao, Angew. Chem. Int. Ed. 39 (2000) 2928.
[61] Y. Shu, D. Ma, X. Liu, X. Han, Y. Xu, X. Bao, J. Phys. Chem. B 104 (2000) 8245.
[62] D. Ma, Y. Shu, X. Han, X. Liu, Y. Xu, X. Bao, J. Phys. Chem. B 105 (2001) 1786.
[63] D. Zhou, D. Ma, X. Liu, X. Bao, J. Mol. Catal. A 168 (2001) 225.
[64] P. Qiu, J.H. Lunsford, M.P. Rosynek, Catal. Lett. 48 (1997) 11.